

Parametric Erosion Investigation: Propellant Adiabatic Flame Temperature

P.J. Conroy, P. Weinacht and M.J. Nusca

US Army Research Laboratory, Aberdeen Proving Ground, MD 21005-5066

ABSTRACT

The influence of quasi-independent parameters and their potential influence on erosion in guns have been investigated. Specifically, the effects of flame temperature and the effect of assuming that the Lewis number (ratio of mass-to-heat transport to the surface), $Le = 1$, has been examined. The adiabatic flame temperature for a propellant was reduced by the addition of a diluent from a high temperature of 3843 K (similar to that of M9) down to 3004 K, which is near the value for M30A1 propellant. Mass fractions of critical species at the surface with and without the assumption of $Le = 1$ are presented, demonstrating that certain species preferentially reach the surface providing varied conditions for the surface reactions. The results for gun tube bore surface regression qualitatively agree with previous studies and with current experimental data. The propellant composition influence upon erosion must still be inferred at this time from the presence of specific product species at the surface because the finite-rate gas surface reactions are not well known under ballistic conditions.

Keywords: Adiabatic flame temperature, gun erosion, propellant composition, surface regression, gun tubes

1. INTRODUCTION

The inner surfaces of most gun tubes regress as a result of various mechanisms, such as mechanical abrasion, pyrolysis, melting, spalling, etc., when the gun is fired. Historically, the propellant adiabatic flame temperature (obtained from Gibbs free energy minimisation with constant volume and no heat loss) has been considered to be the most important factor in determining erosivity¹⁻³. Previous modelling and experimental efforts have not identified the fundamental cause of erosion, and some discrepancies were found between flame-temperature correlations^{4,5}; the discrepancies were not resolved. Attempts to model erosion using first principles have been and are currently being made⁶⁻⁹, although it is believed that significant additional research is still required to understand the fundamental physics involved. In this study, the influence of propellant flame temperature on erosion is analysed as an initial step toward understanding the principle components of the erosion problem in a parametric fashion.

The contributions due to mechanical wear and abrasion are not included in the study, nor are the effects of altered material composition on the surface. Instead, this study focuses on the surface (thermochemical portion) of erosion using full-equilibrium thermochemistry, independent heat transport, and multicomponent species mass transport to the surface.

2. EROSION MODEL DESCRIPTION

The basic outline and new additions to the US Army Research Laboratory erosion physics test model are elaborated upon here for completeness^{8,9}. The model consists of three fully coupled portions comprising (i) thermal ablation/heat transfer/ conduction, (ii) mass transport, and (iii) thermochemistry. The code uses the gas-phase properties in the core flow of the gun tube from XKTC¹⁰, and certain data from IBBLAKE¹¹⁻¹³. The thermochemistry is assumed to be full-equilibrium chemistry and incorporates the NASA Lewis¹⁴ database. New additions to the model include:

- (a) Variable surface physical properties, conductivity $k(T)$, and specific heat $C_p(T)$
- (b) Surface material phase change from body-centred cubic (BCC) to face-centred cubic (FCC) (the material replenishment section recognises the surface temperature and the correct phase)
- (c) A user-defined freeze-out temperature that deactivates the surface chemistry
- (d) An iterative procedure that provides convergence for surface-control volume temperature (the gas and solid specific heats are temperature-dependant and require iteration for convergence)
- (e) All user-defined primary inputs (i.e., no hard-wire input and case-to-case consistency).

The model considers both melting and pyrolysis from surface chemistry. Conceptually, as shown in Fig. 1, the surface heats through convection until the chemical activation temperature is overcome. At this point, surface reactions are permitted to occur, releasing additional energy into the system as a source term at the surface and producing appropriate gaseous, solid, or liquid products.

The reaction products can either remain as some solid materials or be removed from the area as liquids

or gases. The later case results in pyrolysis or ablation. As the surface regresses, the solids are refreshed accordingly. Assumptions made in the erosion models are:

- (a) One-dimensional (1-D) heat conduction
- (b) No subsurface chemical diffusion or reactions
- (c) Instantaneous removal of all surface liquids and gas products
- (d) No feedback to the interior ballistics calculation in the core flow
- (e) Release and treatment of chemical energy as a surface source term
- (f) Freezing of species (i.e., no chemical reactions) from the core flow to the wall

The surface energy balance (when there is no melting) consists of the convective heat input to the surface, along with the possible contribution due to the surface reaction, shown in Eqn (1), where T is the wall temperature, k is the thermal conductivity, and h is the convection coefficient¹⁵. This source term is balanced with the energy conducted through the material as:

$$h(T_{gas} - T_{wall}) = -k \frac{\partial T}{\partial r} - Source \quad (1)$$

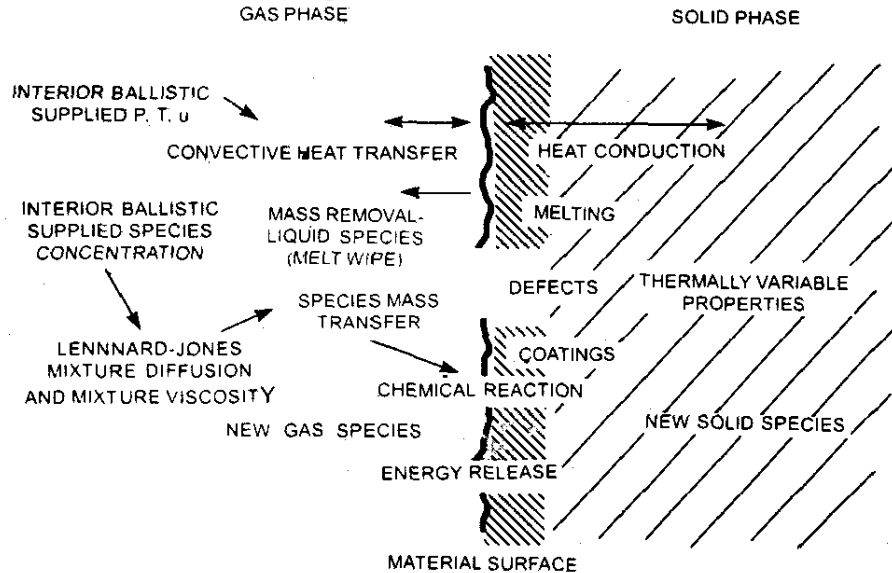


Figure 1. Conceptual erosion model

However, when the system is melting, the energy balance also includes the fixed-surface temperature condition (because the temperature cannot rise beyond this value as the material is removed as fast as it melts and additional energy is preferentially used for more phase transition), as well as the latent heat of formation of the molten material, as shown in Eqns (2) and (3).

$$T_{wall} = T_{melt} \quad (2)$$

and

$$\rho L \frac{\partial s}{\partial t} = h (T_{gas} - T_{wall}) + k \frac{\partial T}{\partial r} + \text{Source} \quad (3)$$

In Eqn (3), L is the latent heat of formation, ρ is the density of the surface material, and s represents the instantaneous surface location that must be iterated upon for convergence until the energy balance is satisfied.

3. CALCULATION METHODOLOGY FOR FLAME TEMPERATURE STUDY

The calculations presented in this study were initiated with a BLAKE¹¹ calculation of a notional propellant having an adiabatic flame temperature of 3843 K. This particular baseline propellant (an altered JA2) was chosen because it had an exceptionally high adiabatic flame temperature, as well as it previously experimentally demonstrated erosivity⁹. The basic charge configuration had a notional slab geometry. The propellant flame temperature was reduced from the nominal value by adding a diluent nitrogen to the nominal gas mixture in increasing mass percentages (15 %, 30 %, and 60 %) without reducing the other components' mass fractions. As a result, the final percentage of diluent added was somewhat less than stated previously, as shown in Table 1.

Using these formulations for the propellants with reduced flame temperature, ranging from 3843 K down to 3004 K, iterations were performed for the XKTC calculations, which involved altering the propellant mass and web, such that the projectile muzzle velocity, muzzle energy, and the peak pressure in the gun were kept constant for all the four scenarios. The results were used in the IBBLAKE calculations. These calculations involved many iterations to determine the combination of projectile mass, propellant mass, and web size which produced the desired results, while maintaining a burn-out condition at projectile exit. Although the total charge mass is changed for each permutation (Table 1), this effect is accounted for in the results. The resulting information involving the gun tube core flow gas composition, temperature, pressure, and velocity for the four different scenarios was then used as input for the calculations.

4. RESULTS

Shown in Figs 2-5 are gun tube, inner-surface temperatures for three of the four notional propellant formulations (Table 1) at three axial locations along the gun tube wall, measured from the rear face of the tube at 635 mm, 686 mm, and 1040 mm, respectively. The initial location of the base of the projectile is 559 mm. The flat areas at the top of the curves in Figs 2-4 are due to the surface temperature reaching a user-defined, surface melt temperature. What is seen in this data is the general reduction from the high, overall temperatures in Fig. 2 to the lower temperatures in Fig. 5.

The slight increase in the recession in Fig. 6 before 3.5 ms and after 4.5 ms in the curves

Table 1. Calculation matrix to investigate the effect of flame temperature

M256 ^a with a 3.629 kg projectile (N ₂ %)	Muzzle velocity (m/s)	Peak pressure (MPa)	Propellant mass (kg)	Mole (Carbon percentage)	Mole (Hydrogen percentage)	Mole (Oxygen percentage)	Mole (Nitrogen percentage)	Adiabatic flame Temp (K)
RPD 351 nominal	1537.0	453.0	6.074	19.694	27.406	40.794	11.932	3843
+ 15	1544.1	451.9	6.346	17.634	24.539	36.526	21.145	3603
+ 30	1542.2	453.4	6.623	15.964	22.215	33.067	28.613	3384
+ 60	1538.9	456.7	8.165	13.422	18.677	27.801	39.981	3004

^a Assumed nonchromium electroplated M256 tank cannon

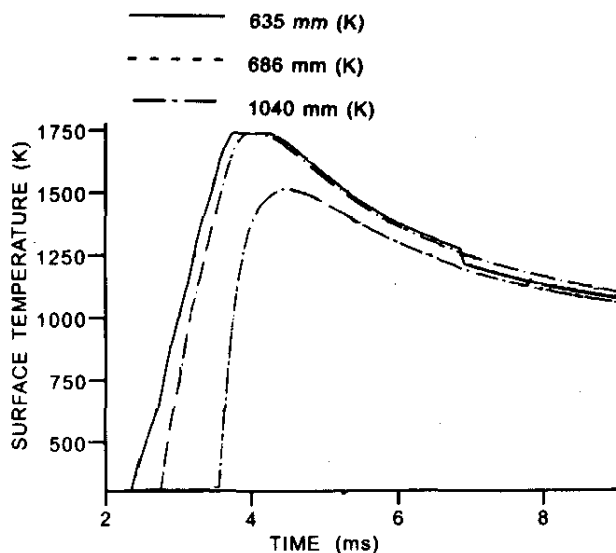


Figure 2. Gun tube surface temperatures for three axial locations and a single firing of a charge having a propellant adiabatic flame temperature of 3843 K.

is due to the pyrolysis, which is also included in the total mass loss and intended for a follow-on study. In Fig. 7, both experimental and numerical data are presented as normalised erosion (surface regression) per round fired versus adiabatic flame temperature. The experimental data include some data from a

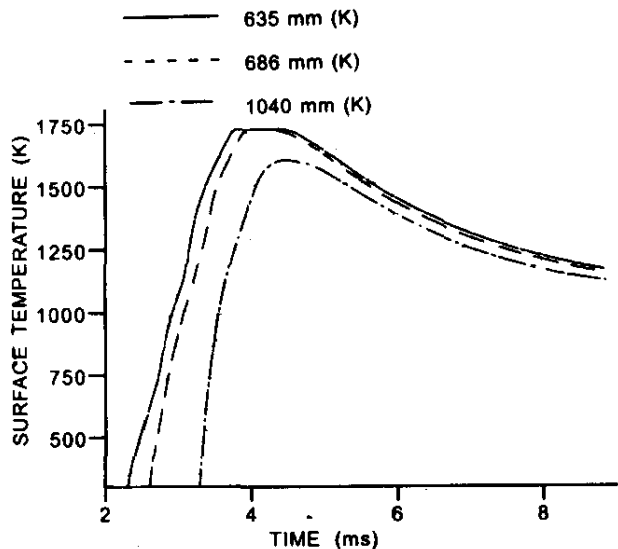


Figure 3. Gun tube surface temperatures for three axial locations and a single firing of a charge having a propellant adiabatic flame temperature of 3603 K.

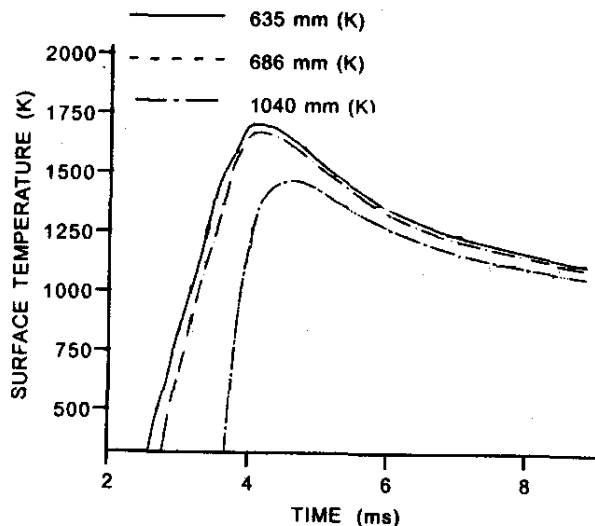


Figure 4. Gun tube surface temperatures for three axial locations and a single firing of a charge having a propellant adiabatic flame temperature of 3384 K.

study presented by Ahmad¹⁶ concerning 5 in./54 gun tube erosion data, as well as Kruczynski's¹⁷ M199 M203A1 origin of rifling wear data per round and the original version of the M919 25 mm round average wear per round at the origin of rifling¹⁸.

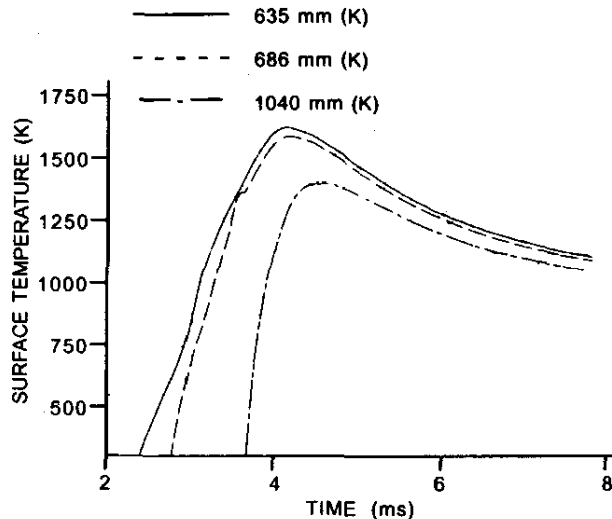


Figure 5. Gun tube surface temperatures for three axial locations and a single firing of a charge having a propellant adiabatic flame temperature of 3004 K.

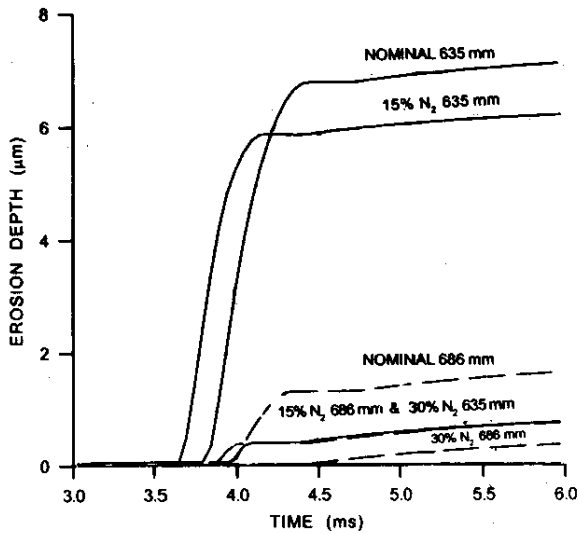


Figure 6. Computed single-shot erosion depths versus time for propellant flame temperatures of 3843 K; 3603 K; and 3384 K at three axial locations each.

Ahmad's data include two different experimental data sets for a 5 in./ 54 system. The values with higher erosion are for a series of firings without coolant additives in the charge, while a series

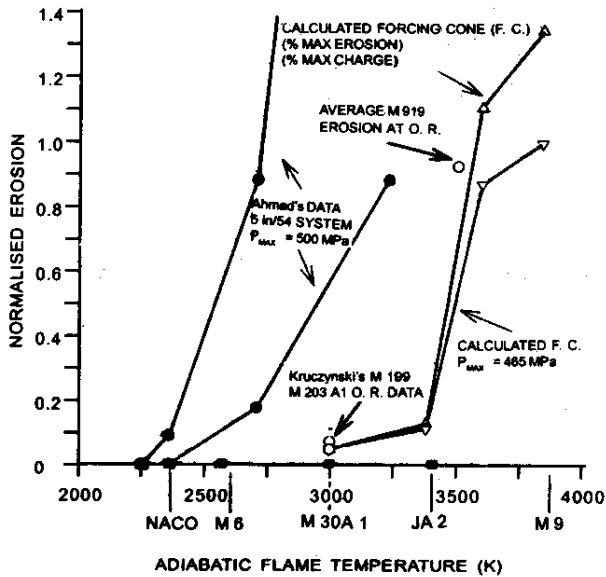


Figure 7. Computed and experimental normalised erosion per round versus adiabatic flame temperature. The numerical calculations are also normalised for charge mass effects. The adiabatic flame temperature for various propellants is shown for reference.

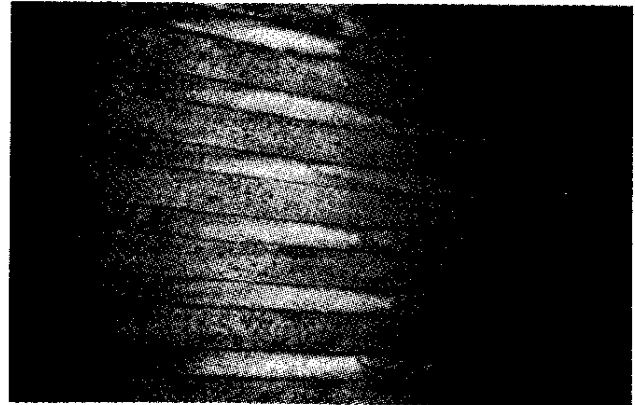


Figure 8. Origin of rifling of 155 mm howitzer showing pyrolysis, loss of chrome, and rifling degradation.

presented with lower erosive values included a talc wax liner in the charges to reduce the overall heat transported to the gun tube wall. Ahmad's data are from one of the few historical studies to vary the flame temperature while attempting to keep all other variables fixed.

The results of his study are experimental in nature and do not represent any existing system. Kruczynski's data include both horizontal and vertical wear at the origin of rifling to account for the asymmetrical wear pattern seen in some artillery charges. However, both

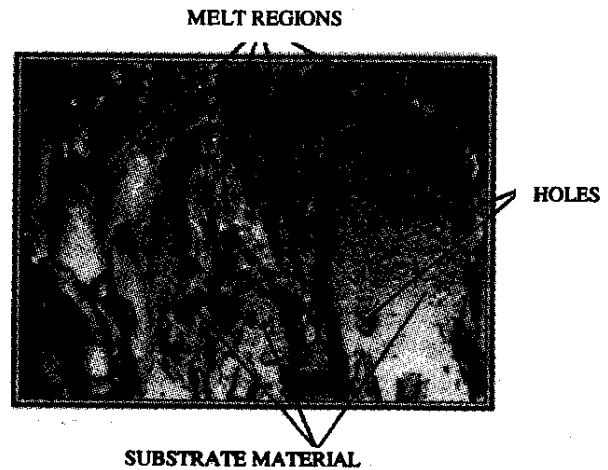


Figure 9. 120 mm M256 tank cannon surface showing chrome stripping, pits, and melt regions.

points are practically coincidental for this plot, including values not shown for the M203 charge. Experimental erosion data is presented in Fig. 7 only to provide some reference points and qualitative behaviour of erosion with the adiabatic flame temperature.

The computed numerical data shown in Fig. 7 consists of two curves of four points each and are plotted as triangles. Both curves have been normalised to the maximum value of computed wear occurring at the 635 mm axial location. The lower of the two curves reflects this normalisation by having one as the maximum value of regression. Due to charge mass modification to maintain constant performance, this computed data was renormalised to incorporate the maximum charge mass, as well as the maximum surface regression (maximum erosion percentage/maximum charge percentage), which resulted in the slightly higher plot. The general trend and values of erosivity versus adiabatic flame temperature seems to be reasonable when compared to the experimental data presented for the 155 mm and 25 mm guns, which has also been normalised for regression. It was noted that the erosion rate accelerates above an adiabatic flame temperature of 3400 K. Protective coatings and charge additives may assist a system operating with an adiabatic flame temperature above this.

While the general regression trend and shape holds for the Ahmad's¹⁶ data, the values appear to be inexplicably shifted by about 700 K, possibly due to the fact that the Ahmad's data was based on firing experimental charges. It was also noted in Fig. 7 that even though no melting occurred for the propellant having the adiabatic flame temperature very close to that of M30A1, the computed surface regression was about that observed by Kruczynski¹⁷ who was firing M30A1 propellant*.

The photograph of an 155 mm howitzer origin of rifling in Fig. 8 shows what type of erosion or pyrolysis can occur at the origin of rifling. It also shows the evidence of heat checking, cracking, and loss of lands; however, there is no obvious evidence of surface melting of this scale as the calculations predicted. Nevertheless, the situation is quite

different for the M256 chromed gun tube as shown in Fig. 9, which fired JA2-type propellant. Evidence of chrome removal, surface pitting and melting are all exhibited in this photograph, as was also expected from the calculations.

Propellant combustion, product species, and molar concentrations are presented in Figs 10 and 11.

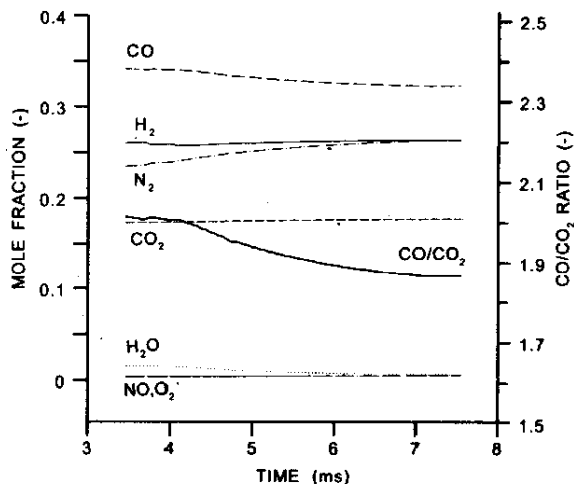


Figure 10. Selected product species mole fractions and CO/CO₂ ratio for gun tube core flow.

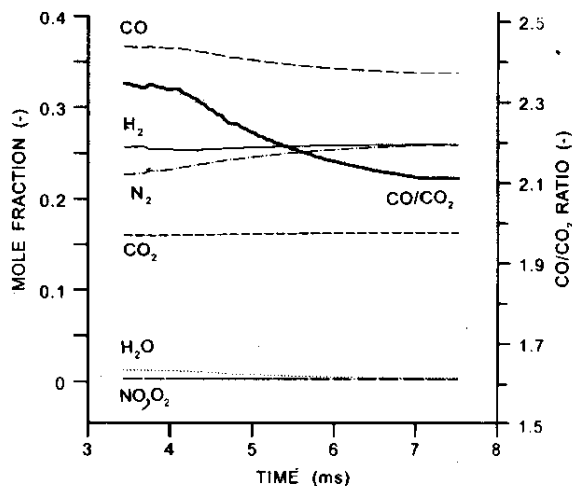


Figure 11. Selected product species mole fractions and CO/CO₂ ratio for gun tube surface.

* The pyrolysis products and related effects are an area of a follow-on study that will investigate the products that the equilibrium chemistry calculation indicates and what actually is being removed from the surface.

The differences between the core flow product species in Fig. 10 and the wall surface product species in Fig. 11 illustrate the effect of multicomponent mass transport upon the species concentration at the surface. The species principally affected using nominal propellant by the mass transport are CO and CO_2 . The concentration in the core flow appear to contain less CO and more CO_2 than at the wall, where the concentration of CO is more and that of CO_2 is less. The CO/CO_2 varies approximately 15 per cent between these regions. This ratio is thought to be very important¹⁹⁻²³.

Fundamental studies are underway to investigate mechanisms in which free carbon may be formed from either CO or CO_2 . Eventually, the primary surface reactions and rates will be known and included in the surface reaction models. The proper state and species concentrations will be required to provide results based on experimentally validated physical processes.

5. CONCLUSIONS

Flame temperature effects on erosion have been studied with four notional computational charges with the assumed gun tube properties for an M256 non-electroplated cannon. These four notional charges had propellant adiabatic flame temperatures 3843 K, 3603 K, 3384 K, and 3004 K. While the trends in erosion match those of Ahmad, the actual values agree better with recent system data, specifically, recently measured data from the 155 mm M203A1 charge and 25 mm M919 round erosion.

Differences in species concentrations exist between the core flow and wall region. This difference may be critical in providing the correct input for chemical reactions at the surface, but as of yet, the actual kinetic mechanisms of erosion at the surface remain unknown. Further parametric investigations of this type are needed to provide an understanding of the interactions of the thermal and chemical, with the ultimate inclusion of mechanical, components as well to erosion/wear. Also, this type of investigation provides guidance for further fundamental studies.

REFERENCES

1. Fisher, E.B. Heating and wear environment. Proceedings of the Workshop on Gun Tube Heating and Erosion. US Army Research Laboratory, Sagamore, Wilmington, DE, July 1996.
2. Caveny, L.H. Steel erosion produced by double-base, triple-base, and RDX composite propellants of various flame temperatures. US Army Armament Research and Development Centre, Picatinny Arsenal, NJ, October 1980. Report No. ARLCB-CR-80016.
3. Lawton, B. Thermal and chemical effects on gun barrel wear. Proceedings of the 8th International Symposium on Ballistics, Vol. 2. Orlando, FL, October 1984, pp. 27-36.
4. Watervliet Arsenal. Proceedings of the Interservice Technical Meeting on Gun Tube Erosion and Control. Watervliet, NY, 25-26 February 1970.
5. Proceedings of the Tri-Service Gun Tube Wear and Erosion Symposium. US Army Armament Research and Development Centre, Dover, NJ, March 1977.
6. Evans, M.R. Transient boundary layer integral matrix procedure TBLEMP users manual. Mountain View, CA, October 1974. Aerotherm UM-74-55.
7. Dunn, S.; Coates, D.; Nickerson, G.; Sopok, S.; O'Hara, P. & Pfligl, G.A. Unified computer model for predicting thermochemical erosion in gun barrels. Proceedings of 31st AIAA/ ASME/ SAE/ ASEE Joint Propulsion Conference and Exhibit, San Diego, CA, July 1995. Paper No. AIAA 95-2440.
8. Weinacht, P. & Conroy, P.J. A numerical method for predicting thermal erosion in gun tubes. US Army Research Laboratory, Aberdeen Proving Ground, MD, July 1996. Report No. ARL-TR-1156.
9. Conroy, P.J.; Weinacht, P. & Nusca, M.J. Surface chemistry effects on high performance tank ammunition. US Army Research Laboratory,

- Aberdeen Proving Ground, MD, October 1997. Report No. ARL-TR-1526.
10. Gough, P.S. The XNOVAKTC code. US Army Ballistic Research Laboratory, Aberdeen Proving Ground, MD, February 1990. Report No. BRL-CR-627.
 11. Freedman, E. BLAKE—a thermodynamic code based on Tiger: Users guide and manual. US Army Ballistic Research Laboratory, Aberdeen Proving Ground, MD, July 1982. Report No. ARBRL-TR-02411.
 12. Anderson, R.D. & Fickie, K.D. IBHVG2—a users guide. US Army Ballistic Research Laboratory, Aberdeen Proving Ground, MD, July 1987. Report No. BRL-TR-2829.
 13. Janke, P.J.; Dyvik, J.A. & Marksberry C.L. Electrothermo-chemical propellant extensions to the IBHVG2 interior ballistics simulation: Model development and validation. *In* CPIA Publication No. 620, Vol. 3, October 1994, pp. 171–81.
 14. Gordon, S. & McBride, B.J. Computer program for calculation of complex chemical equilibrium compositions, rocket performance, incident and reflected shocks, and Chapman-Jouget detonations. NASA Lewis Research Centre, Cleveland, OH, 1971. Report No. NASA SP-273.
 15. Conroy, P.J. Gun tube heating. US Army Ballistic Research Laboratory, Aberdeen Proving Ground, MD, December 1991. Report No. BRL-TR-3300.
 16. Ahmad, I. The problem of gun barrel erosion: An overview. *In* Gun Propulsion Technology, Vol. 109, Chapter 10, 1988.
 17. Kruczynski, D.L.; Stobie, I.C. & Kummerich, M.B. Gun tube/charge/projectile interactions and gun tube wear. US Army Ballistic Research Laboratory, Aberdeen Proving Ground, MD, June 1989. Report No. BRL-TR 3004.
 18. Talley, J. Q. & Owczarczak, J.A. 25 mm barrel erosivity study. Final report. GenCorp Aerojet Corporation, Aerojet Ordnance Division, Downey, CA, August 1991.
 19. Kamdar, M.H. & Venables, J.D. Characterisation of surface layers in gun barrels. US Army Armament Research and Development Centre, Watervliet, NY, 1984. Report No. ARLCB-TR-84041.
 20. Morphy, C.C. & Fisher, E.B. The role of carburisation in gun barrel erosion and cracking. US Army Ballistic Research Laboratory, Aberdeen Proving Ground, MD, July 1981. Report No. ARBRL-CR-00459.
 21. Morphy, C. C. & Fisher, E. B. Gas chemistry effects on gun barrel erosion: A shock tube investigation. US Army Ballistic Research Laboratory, Aberdeen Proving Ground, MD, June 1982. Report No. ARBRL-CR-00481.
 22. Ringers, D.A. & Danese, J.B (Jr). Quantum chemistry, chemisorption, and erosion I. Properties of diatomic molecules. US Army Ballistic Research Laboratory, Aberdeen Proving Ground, MD, 1977. Report No. BRL-TR-2023.
 23. Weigand, J.H. The application of erosion in vent plugs to recoilless guns. US Army Ballistic Research Laboratory, Aberdeen Proving Ground, MD, 1945. Report No. BRL-MR-340.